Indian J. Met. Hydrol. Geophys. (1975), **26**, 1, 11-28

551.551

Characteristics of natural wind — Pt. II : Turbulent flow

V. KR. SHARAN

Department of Aeronautics,

Royal Institute of Technology, Stockholm

(Received 27 December 1973)

ABSTRACT. The characteristics of wind fluctuations are critically reviewed and analysed in terms of turbulence, intensiy, power spectral density and correlation coefficient. It is shown that root mean square gust speed decreases very slightly with height in the lower part of the boundary layer. Various mathematical models of power spectrum for the three components of the fluctuating wind velocity are critically discussed. It is noted that u- and v-spectra show a greater dependence on the type of the terrain suggesting that meso-scale features are of importance for the low frequency portion. The low frequency portion of u- and v-spectra react to changes in atmospheric stability with the v-spectrum being more dependent than u-spectrum. The w-spectrum follows the similarity theory the most of the three components. The vertical spectrum appears to be dependent on height whereas it is difficult to conjecture in favour of either hypothesis for the horizontal spectra. Correlation coefficient measurements of u- and v-components show that the length scales increase with height. Based on the assumption of Taylor's hypothesis and isotropy, expressions are given for the theoretical prediction of correlation coefficient, coherence and the various length scales. Both analytical and empirical gust factor models are presented and it is shown that the gust factor varies with the averaging time period, the site conditions and the height above the ground.

1. Introduction

Air never flows with a perfectly smooth and streamline motion, but always with fluctuations which, when sudden and relatively brief, are called gusts. These velocity fluctuations are of virtually all time scales, varying from fraction of a second to many days and can become detrimental for present day structures, as evidenced by partial or complete failures of numerous structures in the past. Besides the duration of the gust the dimensions of the gust are also of importance in considerations of wind loading on long structures. For our purpose the instantaneous value of the wind velocity (u) may be expressed as the sum of two terms,

$$u = \bar{u} + u' \tag{1}$$

where $\bar{u}$ represents the mean velocity (its characteristics were discussed in Pt. I) and u' is the fluctuating component whose characteristics are discussed in this paper.

2. Characteristics of atmospheric turbulence

The usual way of representing the character of the wind fluctuations in quantitative terms is the energy spectrum, usually the longitudinal energy spectrum (Fig. 1). $S(n)dn$ represents the mean square value of the velocity flucutations in the bandwidth d_n centred at frequency n. By definition, the total energy of the turbulent fluctuations is given by the intergal of $S(n)$ over the whole range of frequencies, *i.e.*, the total area under the curve,

$$\overline{u'^2} = \int_0^\infty S_u(n)\, dn = \int_0^\infty n\, S_u(n)\, d(\log n) \tag{2}$$

where $S_u(n)$ is power spectrum of u-component and n is frequency in cycles per sec. It is obvious that the wind in the earth's boundary layer consists of fluctuations having characteristic periodicities of the order of a year, several days, a day and a minute. Thus the entire spectrum, may be divided into three regions :

(1) The macrometeorological region associated with large scale air flows—cyclones and anticyclones.

(2) The mesometeorological range which probably accounts for the diurnal wind fluctuations.

(3) The micrometeorological range which represents the true turbulence of the flow, also known as wind gustiness.

The primary production of wind's kinetic energy, derived from the sun through cyclogenesis, takes place at the macrometeorological scales of periodicity of several days, corresponding to the major macrometeorological peak in the wind energy spectrum in Fig. 1. Solar activity accounts for two subsidiary diurnal and annual peaks. The former is associated with diurnal heating and cooling effects and is more apparent near the ground

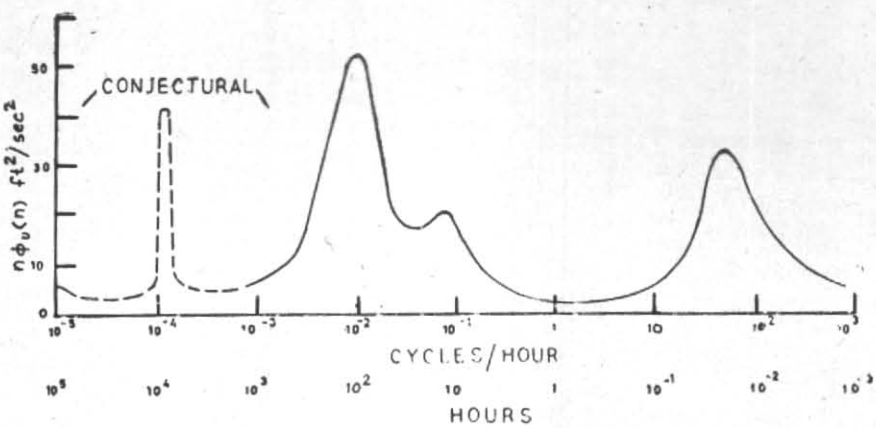

Fig. 1. Spectrum of horizontal wind speed near the surface of the ground

the latter arises from the annual variation in the temperature gradient between the polar and equatorial regions; this is less in summer and mean monthly wind speeds may then be only two-thirds those in winter.

Dissipation of the wind's energy takes place at the micrometeorological frequencies in the natural boundary layer. The shear stresses induced at the earth's surface produce eddies having a scale of a few thousand feet, the engery of which is derived from the mean flow, and cascades down to smaller scale motions to be finally dissipated through viscosity; this is reflected in the micrometeorological spectrum shown in Fig. 1. The peak in the energy appears at a frequency of one cycle per minute in a strong wind and somewhat slower in a moderate wind. The energy level appears to vary directly as the shear stress; consequently the fluctuation amplitudes are proportional to the mean wind strength itself. It should be realized that although a spectrum such as Fig. 1 will only apply to a particular site and a particular height above the ground, the general form of the spectrum and the position of the peaks remain very much the same regardless of the geographical locality, the nature of the terrain and the height above the ground. One of the most important distinctions that can be made is between the fluctuations of a macrometeorological kind, *i.e.*, weather map fluctuations, and micrometeorogical kind, *i.e.*, gusts. From Fig. 1 it is obvious that the two types of fluctuations are separated by a gap extending from roughly 1 to 10 cycles per hour, to which corresponds a very low energy of fluctuations. This portion of the spectrum is known as the spectrum gap. Its practical interest is justified by the fact that if the wind speed is averaged over any length of time included within this gap the value so obtained is essentially constant. From this follows the current practice of using a sampling time between 10 minutes and 1 hour to evaluate the mean wind speed. Fig. 1 is based partly on the data of Van der Hooven (1957).

Looking at the lower frequency end of the spectrum from a statistical stand-point, a given mean wind speed can be associated with its return period, that is the number of days or years between two occurrences of the same wind speed in relation to the expected lifetime of the structure. On the other hand, the shape of the curve at the high frequency end of the spectrum means that the mean velocity is likely to be considerably exceeded for any period of time shorter than 10 minutes, say a few seconds. If the duration of each gust is long enough, it allows both the wind loads to develop and the structure as a whole to deflect. It is this aspect of natural boundary layer, namely the characteristics of the turbulent fluctuations in the wind, also called gusts, which is discussed below. A knowledge of turbulent properties is required not only for the analytical determination of the dynamic response of structures to gusts, but also for the correct wind tunnel modelling of turbulence.

Turbulent fluctuations of the wind (gusts) can be best studied using the methods developed for the treatment of randomly fluctuating signals, encountered in communications and control engineering. We assume that the gust fluctuations about the hourly mean wind speed constitute a stationary random process and that the gusts are dependent only on two parameters, the average wind speed and the surface roughness. Further, we will ignore any systematic change of mean wind direction.

The gusts vary both in space and time very rapidly and may be written as,

$$\underline{v} = \underline{v}\,(x, y, z; t) \tag{3}$$

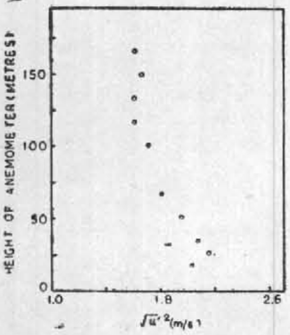

Fig. 2. Variation of r.m.s. gust speed with height over Rugby —

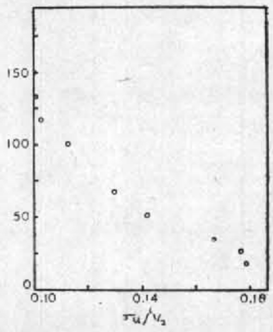

Fig. 3. Turbulence intensity measurements over Rugby

where $\underline{v}$ is total fluctuating velocity.

However, we will only study the Eulerian characteristics, *i.e.*, the time average properties at one point of observation and, therefore, we may write the gust velocity in component form,

$$\underline{v}(t) = \left[u'(t), v'(t), w'(t) \right] \tag{4}$$

with the gust speed being defined as,

$$\left| \underline{v}(t) \right| = \left[u'^2(t) + v'^2(t) + w'^2(t) \right]^{\frac{1}{2}} \tag{5}$$

where u', v' and w' are fluctuating wind speed in x,y and z directions. The root-mean-square (r.m.s.) gust speed $\sigma(\underline{v})$ is defined by,

$$\sigma^2(\underline{v}) = \frac{1}{T}\int_0^T \left| \underline{v}(t) \right|^2 dt$$

$$= \frac{1}{T}\int_0^T \left[u'^2(t) + v'^2(t) + w'^2(t) \right] dt$$

$$= \sigma^2(u) + \sigma^2(v) + \sigma^2(w) \tag{6}$$

where $\sigma(u)$, $\sigma(v)$, $\sigma(w)$ are variance of u, v and w components of fluctuating velocity.

Near to the ground level, $\sigma(u) \sim 3\sigma(v)$ and $\sigma(w)$ is still smaller, so that the conventional instruments, sensing only $u'(t)$ do provide a good approximation to $\sigma(v)$.

Fig. 2 shows the variation of r.m.s. gust speed with height over Rugby. It is obvious that the r.m.s. gust speed decreases very slowly with height. Physically, the turbulence and hence the gust speed must tend to zero at heights approaching the gradient heights. Assuming that the r.m.s. gust speed is invariant and equal to the value measured at 10 metres above the ground level, Harris (1970) showed, it may be related to the mean wind velocity by,

$$\sigma(u) = 2.58\, K^{1/2}\, V_{10} \tag{7}$$

K=Surface drag coefficient, V_{10}=Mean wind speed at height 10m. From Fig. 5 (Pt. I) V_{10}=10·35 m/s and taking K=0·006 corresponding to Rugby terrain, we get $\sigma(u)$=2·07 m/s, showing good agreement with the measured value. Harris (1970) showed that r.m.s. gust speed is virtually independent of height; a reasonable value of $\sigma(u)$ based on values of V_g, z_g (subscript g shows geostrophic value) and K suggested in Table 2 (Pt. I) is given by,

$$\sigma(u) \simeq 0.11\, V_g \tag{8}$$

or,

$$\sigma(u) \simeq 0.19\, V_{10} \tag{9}$$

The ratio $\sigma(u)/V_z$ is called the intensity of turbulence. Since $\sigma(u)$ is almost invariant with height, it follows that the intensity of turbulence decreases with height, mainly because the mean wind speed increases. It may be written as,

$$\sigma(u)/V_z = 2.58\, K^{1/3} (10/z)^{\alpha} \tag{10}$$

Fig. 3 shows the results of turbulence intensity measurements over Rugby. Using the value of V_{10} from Fig. 5 (Pt. I) and from Eqn. (10) we get for $\sigma(u)/V_z$=0·17, in agreement with the measured results.

Although turbulence in the atmosphere is generally both convective and mechanical in origin, in high winds convective turbulence plays a relatively minor role. The reason for this is, whereas mechanical turbulence rapidly increases in intensity with wind speed, convective turbulence tends to be damped out by the powerful mixing action caused by the mechanical turbulence; the latter prevents the necessary thermal instabilities from arising and tends to reduce the amosphere to a state of neutral stability. This almost complete predominance of mechanical turbulence suggests that in high winds the turbulence intensity near the ground will only vary significantly with the mechanical drag forces between the air and the ground and the height. The influence of these factors on the frequency-wise distribution of turbulent energy in the wind is now discussed.

3. The behaviour of the variances in terms of similarity parameters

According to Monin-Obukhov similarity theory, the non-dimensional variances, namely, $\sigma(u)/u_*$, $\sigma(v)/u_*$, $\sigma(w)/u_*$ are functions of R_i or z/L only (since z/L is a universal function of R_i in the surface layer). Here $u_*(=\sqrt{\tau_0/\rho})$ is the friction velocity, R_i is the Richardson number and L is a scaling (Monin-Obukhov) length, defined as,

$$L = -\frac{u_*^3\, c_p\, \rho\, T}{g\, k\, H} \tag{11}$$

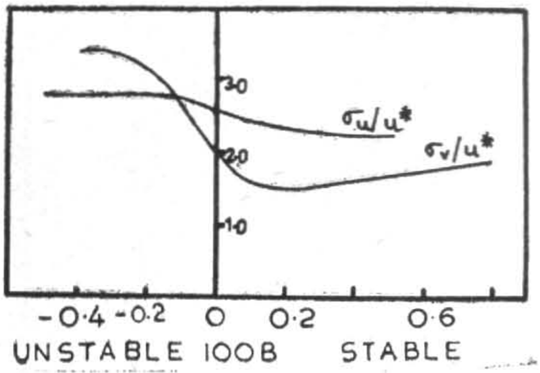

Fig. 4 (a). The ratios σ_u/u_* and σ_v/u_* based upon results from many sources. Confidence intervals represent standard deviation of mean, assuming all observations are independent of each other

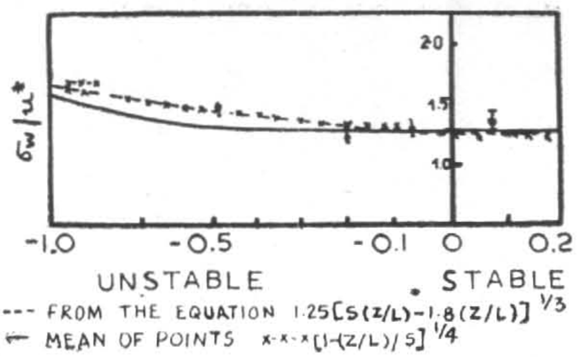

Fig. 4 (b). σ_w/u_* based upon results from many sources

where c_p=Specific heat of air at constant pressure, ρ= Air density, T= Absolute temp., g= Acceleration due to gravity, k=Von Karman constant and H=Vertical turbulent heat flux (positive upward).

Fig. 4 shows these relationships from many observations (Prasad & Panofsky 1967). The rations $\sigma(u)/u_*$, $\sigma(v)/u_*$ show systematic variations from place to place, suggesting that terrain features of large scales than those characterized by z_0 influence their behaviour. Furthermore, $\sigma(v)/u_*$ shows an increase for large R_i, suggesting the existence of small-scale, horizontal motions besides mechanical turbulence and heat convection. The Monin-Obukhov prediction fits best to the statistics of vertical velocity. Over the range $-0{\cdot}5< R_i <0{\cdot}2$, $\sigma(w)/u_*$ is essentially constant and equal to $1{\cdot}3$. For negative R_i of large magnitude $\sigma(w)/u_*$ varies as $(z/L)^{1/3}$.

In general there is very little vertical variation of the variances in the surface layer. Besides, the various ratios are relatively unaffected by terrain heterogeneties.

4. The spectrum of gust velocities

According to Monin-Obukhov similarity theory, the spectrum of a velocity component in the surface layer is given upto a height of about 50 m by,

$$\frac{n\,S(n)}{u_*^{\,2}} = F\,(f\,,z/L) \tag{12}$$

where $S(n)$ = Spectral density at frequency n,
f = Nondimensional frequency $(= nz/\bar{u})$.

The observations of vertical velocity agree quite well with Eqn. (12). The lateral component, however, does not appear to follow the above similarity law closely. The behaviour of longitudinal component is intermediate between that of vertical

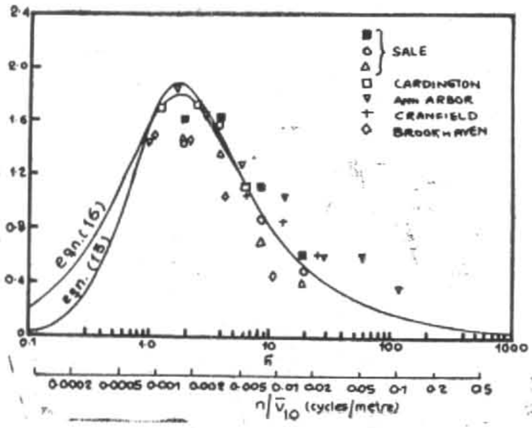

Fig. 5. Spectrum of horizontal gustiness in high winds

and lateral components. The detailed spectra of individual components are discussed below.

5. Spectrum of horizontal gustiness

The spectrum of horizontal wind speed over an extended frequency range was referred to in Fig. 1. The high frequency end of the spectrum, also called the micro-spectrum, determining the nature of the gusts is looked into greater detail below.

A complete description of the average spatial and temporal properties of gusts would require a knowledge of the relationship of each of the three velocity components at one point in space to the corresponding components at some other point. From the viewpoint of wind loading of structures, probably the most important power spectrum is that of the longitudinal component since this gives rise mainly to the fluctuations in drag. However, in tall structures, the lateral component can also contribute to the lateral fluctuations and in bridge decks the vertical component of velocity can give rise to an important and somewhat unexpected lift force (Davenport 1962).

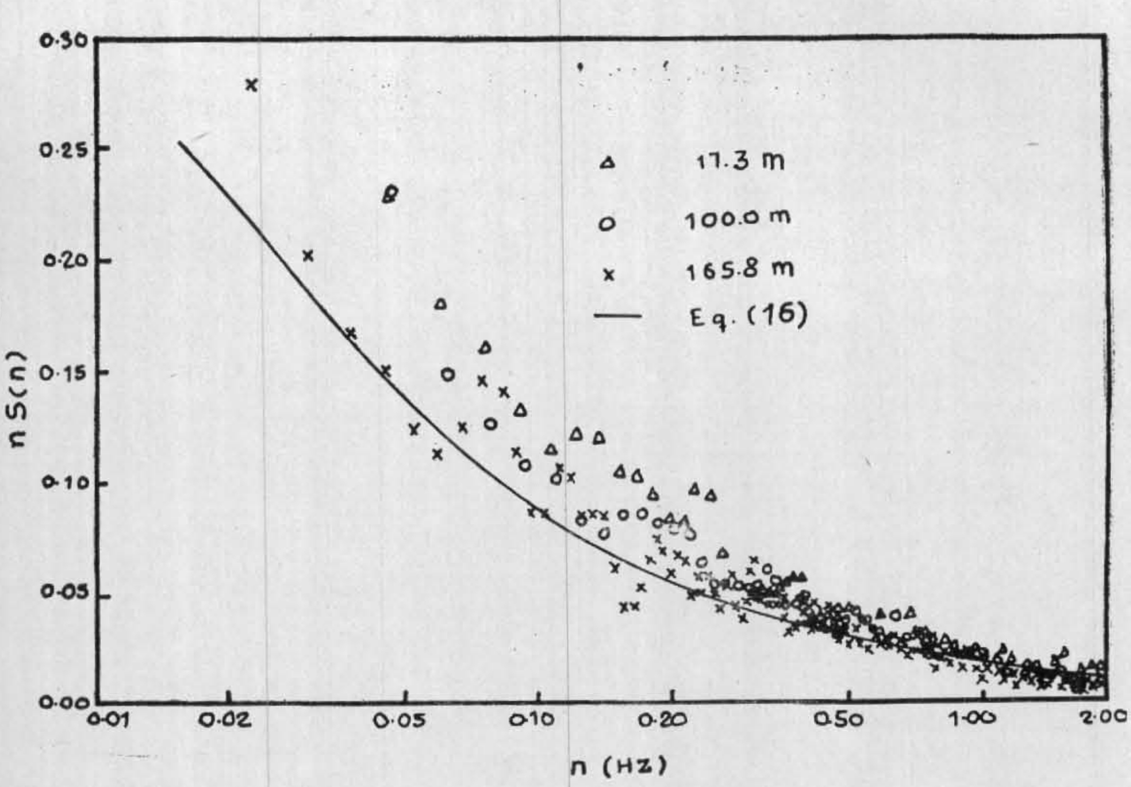

Fig. 6. Power spectrum for u-component at different heights over Rugby

Power spectrum provides a description of the evolution of the random gust velocity with time. Fig. 5 shows measured spectra over different sites of varying roughness and height. At high mean wind speeds the spectral peak appears to exist at wave numbers between 0·001 and 0·002 cycles m^{-1} and the peak wave-length appears to be independent of the type of surface, a fact also confirmed by Deland and Panofsky (1957). At the high frequency end of the spectrum (wavelengths less than observation height) the eddies appear to belong to the inertial subrange of frequencies. These eddies acquire energy only by the decay of larger eddies and lose energy only by transfer to smaller eddies; the various forces are insignificant and the average properties are determined solely by the average rate of dissipation of energy per unit mass of the fluid.

Based on the data of Fig. 5 Davenport (1961) suggested the following expression for horizontal gustiness,

$$\frac{n\,S_u\,(n)}{K\;V_{10}^{\,2}} = 4.0\;\frac{x^2}{(1+x^2)^{4/3}} \qquad (13)$$

where $S_u\,(n)$ is the spectrum of horizontal speed at frequency n and height z and $x = \mathbf{L}n/V_{10}$ where n/V_{10} is in waves per metre, and $\mathbf{L}$ is a scale length of the order of 1200 metres. The expression is also shown in Fig. 5. Following feature should be noted. Almost all the engergy is confined to wavelengths less than 2000 or 3000 metres. The spectrum is proportional to $KV_{10}^{\,2}$, which itself is proportional to the shear stress between the air and the ground. The spectrum is proportional to $(n/V_{10})^{-2/3}$ for large values of n/V_{10}.

Since the mean-square fluctuation is proportional to the area under the spectrum it follows that the turbulence intensity at height z is,

$$\sigma(u) = \left[\int_0^{\infty} S_u(n)\,dn\right]^{\frac{1}{2}} \Big/ V_z$$

$$= 2.35\;K^{1/2}V_{10}/V_z$$

$$= 2.35\;K^{1/2}(z/10)^{-\alpha}$$ (Using the power law expression for mean velocity profile).

This shows that both the turbulence intensity and the power spectrum are independent of wind velocity and dependent only on the height and the roughness parameter of the terrain.

It is obvious that the peak of $nS_u(n)$ spectrum occurs within a band of frequencies. Until recently the bulk of evidence seemed to point to a slight systematic increase of $\bar{u}/n_m$ in the first 100 m (Berman 1965, Bush and Panofsky 1968). However, the latest analysis by Fichtl and McVehil (1969) of data from a 150 m NASA tower in Florida fails to show any such systematic variation.

As regards the variation of $\sigma(u)$ with height, the similarity argument implies constancy, in keeping with the effective constancy of u_* with height. For height over which the fall of u_* may no longer be neglected, $\sigma(u)$ remains proportional to u_* (Panofsky 1962). This means that (on a given site) the change in $\sigma(u)$ between two levels should be proportional to the wind speed (at a given height). Values of $\sigma(u)/u_*$ on various sites range from $2 \cdot 1$ to $2 \cdot 9$.

In the high frequency region, there is sufficient evidence that the u-component spectrum fits closely to the expected variation with frequency, which is,

$$S_u(n) = C\bar{u}^{2/3}\epsilon^{2/3}n^{-5/3} \tag{14}$$

where the universal constant $C \simeq 0 \cdot 14$ (n in Hz). This follows from the reasoning that the small scale properties must be related uniquely to the rate of dissipation of turbulent kinetic energy ϵ. It is known that for low heights the $-5/3$ region of the u-component spectrum appears to hold for wave-lengths upto several times the height. Panofsky (1969) suggests that ϵ may be obtained even in unstable conditions from,

$$\epsilon = \frac{u_*^3}{kz}(\phi_m - z/L) \tag{15}$$

where ϕ_m= Monin-Obukhov stability function for momentum.

In practice, especially at low levels, $\epsilon kz/u_*^3$ appears to change little from unity as instability is increased, which may reflect a compensation from the diffusion term neglected in Eqn. (15). Observations quite close to the ground often suggest less energy in the vertical velocities than in the longitudinal velocities at high frequencies. Bush and Panofsky (1968) mention that the $-5/3$ law for the lateral components exist only as long as the height is at least 7 times the wave-length. In other words, local isotropy exists only for wave-lengths much shorter than often assumed, and for wave-lengths much shorter than those for which the horizontal velocity components obey the Kolmogorov law for the inertial subrange.

Harris (1970) proposed an improvement to Davenport's expression which is given below,

$$\frac{nS_u(n)}{K\,V_{10}^2} = \frac{4x}{(2+x^2)^{5/6}} \tag{16}$$

This is also shown plotted in Fig. 5 More recent results suggest that $L \approx 1800$ metres.

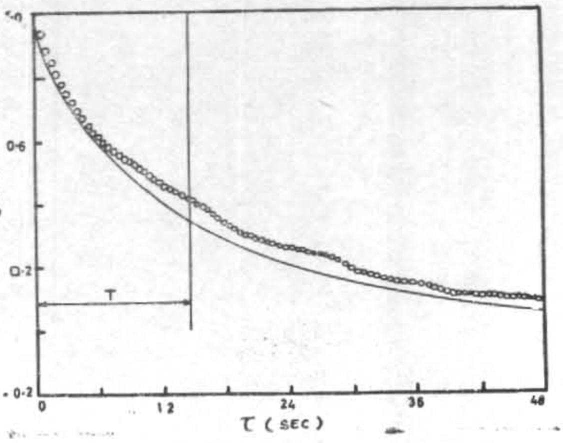

Fig. 7. Auto-correlation function for u-component from measurements at 165·8 m over Rugby, Eqn. (20)

Harris' measurements of power spectrum of longitudinal component over Rugby for three different heights are shown in Fig. 6 along with Eqn. (16). Apart from the natural scatter at the lower end of the frequency scale, the three experimental spectra are consistent with the proposal that the spectrum is invariant with height. The shape of the predicted spectrum is substantially the same as that obtained experimentally.

Another method which can be used to describe the properties of a random signal is through auto-covariance function $C(\tau)$ defined as,

$$C(\tau) = \langle u(t).\, u(t+\tau) \rangle_t$$

$$= \frac{1}{T}\int_0^T u(t).\, u(t+\tau)\, dt \tag{17}$$

(here the notation $\langle\rangle_t$ denotes an average with respect to time). In normalized form, it is called the auto-correlation function $\rho(\tau)$, given by,

$$\rho(\tau) = C(\tau)/C(0) = C(\tau)/\sigma^2(u) \tag{18}$$

$\rho(\tau)$ may be regarded as a quantitative measure of how much information a measurement of the gust component at one instant of time gives about the value which will be measured τ seconds later. In other words, the gust signal, as it evolves in time, has associated with it, a characteristic 'memory time' of time scale T, such that the measurement of signal provides reasonable information about the value τ seconds later if $\tau < T$ and little information if $\tau > T$. T is defined as,

$$T = \int_0^\infty \rho(\tau)\, d\tau \tag{19}$$

where T may be called the average 'memory time' of a gust.

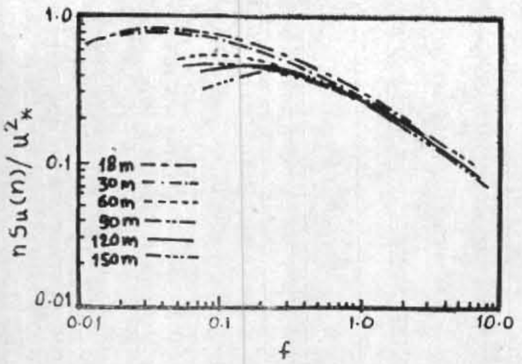

Fig. 8 (a). Diamensionless logarithmic longitudinal spectra for neutral wind conditions plotted in Monin coordinates

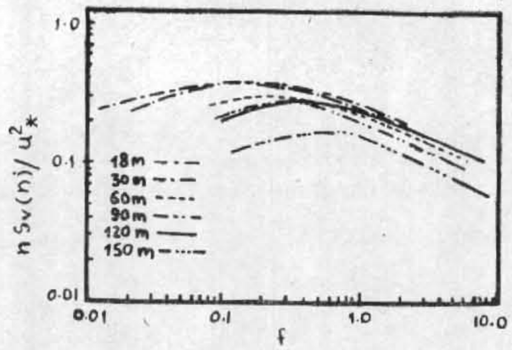

Fig. 8 (b). Dimensionless logarithmic lateral spectra for neutral wind conditions plotted in Monin coordinates

Auto-correlation function for longitudinal component at a height of 165·8 m as measured by Harris over Rugby is shown in Fig. 7. The autocorrelation function and the power spectrum form a Fourier transform pair. Using this relationship, Harris derived the following formula for the auto-correlation function,

$$\rho(\tau) = \frac{2}{\Gamma(1/3)}\left(\frac{\bar{\tau}}{2}\right)^{1/2} K_{1/3}(\bar{\tau}) \qquad (20)$$

where $\bar{\tau}=2\sqrt{2\pi}V_{10}\,\tau/\mathbf{L}$, $\Gamma(1/3)$ has the numerical value $2\cdot679$ and $K_{1/3}(\bar{\tau})$ is a modified Bessel function of the second kind of order 1/3 (Tables of Bessel function of fractional Order, **11**, 1949, Columbia Univ.Press). This is also shown in Fig. 7 and is in good agreement with the experimental measurements. Integrating the above equation we get the time scale of the turbulence (*see* Eqn. 19) as,

$$T = \sqrt{2}\,\Gamma(5/6)/\sqrt{\pi}\,\Gamma(1/3)\mathbf{L}/V_{10}$$
$$= 0.084\mathbf{L}/V_{10} \qquad (21)$$

where $\Gamma(5/6)=1\cdot129$. Note that this time scale is independent of height above ground level.

Fichtl, Kaufman and Vaughan (1970) measured the power spectrum of the longitudinal and the lateral components of turbulence at the Kennedy Space Centre, Florida in neutral wind conditions. They assumed that the similarity theory of Monin (1959) for the vertical velocity spectrum could be applied to the longitudinal and lateral spectra too, so that,

$$nS(n)/u_*^2=F(f,\ R_i) \qquad (22)$$

where F is a universal function of the dimensionless wave number f, given by $nz/\bar{u}$ and the gradient Richardson number R_i. In neutral conditions $R_i = 0$, and for this case Fig. 8 shows the dimensionless logarithmic longitudinal and lateral spectra plotted in Monin coordinates. It is obvious that the position of the maxima shift towards higher values of f as the height increases, implying that Monin coordinates $[nS(n)/u_*^2, f]$ fail to collapse the spectra in the vertical and thus an added height dependence should be included. This has been confirmed by measurements from the tower data from Round Hill (Bush and Panofsky 1968). This may be explained by the fact that the Reynolds stress and the length scale used to scale the wave number $n/\bar{u}$ vary in the vertical direction. However, the data appear to show, that Monin coordinates will collapse spectra with various turbulence intensities at any particular level in the vertical, confirming the earlier observation that the horizontal spectrum is independent of the nature of the roughness of the terrain.

To produce a vertical collaspe of the data, Fichtl *et al.* assumed that the spectra in the Monin coordinates are shape-invariant in the vertical, a reasonable hypothesis permitting a practical approach to developing a spectral model of turbulence.

Fig. 9 (a) shows the vertical variation of the dimensionless wave number f_{mu} associated with the peak of the logarithmic spectrum $S(n)$ along with data from other tower sites. Also shown is the least-square-analysis curve,

$$f_{mu}=0\cdot03(z/18) \qquad (23)$$

where z is in metres. A plot of $nS_u(n)/u_*^2$ *versus* f/f_{mu} will shift the spectra at the various levels, so that all the peaks of the logarthmic longitudinal spectra are located at $f/f_{mu}=1$.

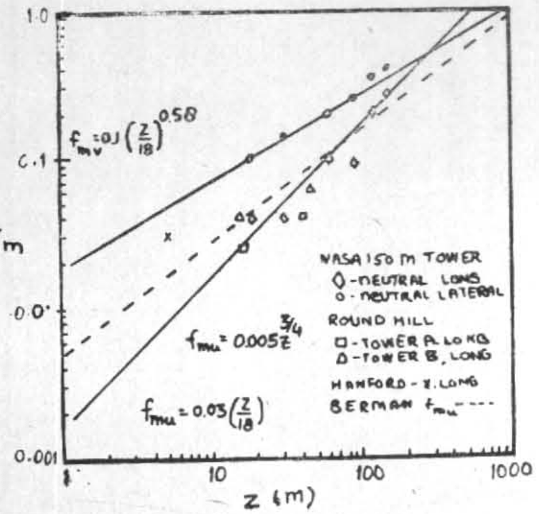

Fig. 9 (a). Vertical distributions of f_{mu} and f_{mv} associated with the peak of the logarithmic u- and v-spectra for neutral stability conditions

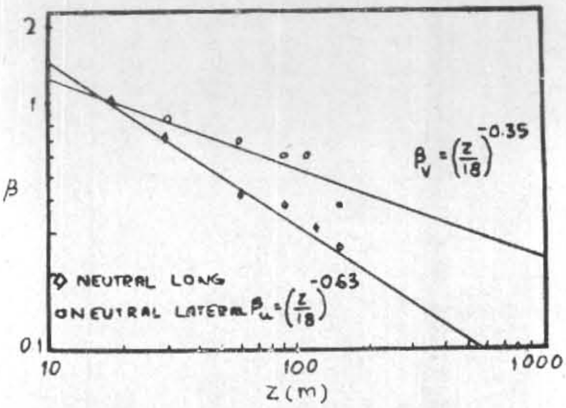

Fig. 9 (b). The vertical distribution of collapsing factors β_u and β_v for neutral stability conditions

The average ratio β_u(vertical collapsing factor for power spectrum for u-component) of the shifted spectrum at level z and the 18-metre spectrum is shown in Fig. 9 (b), along with the least-square-analysis curve,

$$\beta_u = (z/18)^{-0.63} \tag{24}$$

where z is in metres. A plot of $nS_u(n)/\beta_u u_*^2$ *versus* f/f_{mu} will collapse the longitudinal spectra (*see* Fig. 10).

Fichtl *et al.* have suggested the following expression to represent the longitudinal spectrum.

$$\frac{nS_u(n)}{\beta_u u_*^2} = \frac{C_u f/f_{mu}}{[1+1\cdot5(f/f_{mu})^{ru}]^{5/3\,ru}} \tag{25}$$

where C_u and r_u are the constants. Using a least-square-analysis of the data of Fig. 10 $C_u = 8\cdot641$ and $r_u = 0\cdot845$.

Using similar analysis Fichtl *et al.* obtained the following expression for the lateral spectrum,

$$\frac{nS_v(n)}{\beta_v u_*^2} = \frac{C_v f/f_{mv}}{[1+1\cdot5(f/f_{mv})^{r_v}]^{5/3\,r_v}} \tag{26}$$

where $C_v = 8\cdot686$, $r_v = 0\cdot512$ based upon least-square-analysis of the above data. The corresponding data for f_{mv} and β_v is shown in Fig. 9 (b) and Fig. 10 along with the least-square-analysis curves.

It should be noted that u-spectrum shows a greater dependence on the type of terrain (Fig. 11 a). It is obvious that the spectra do not follow similarity theory, and further the shapes of the spectra from various cities differ widely. In particular, the wave-length at the maximum varies considerably from site to site. It is particularly long for cities. This suggests that it is the the meso-scale features that determine the characteristics of the low frequency portions of the u-spectra, and not the roughness length z_0, which is a measure of local roughness. Spectral densities of lateral velocities behave very much as those of longitudinal velocities, only more so.

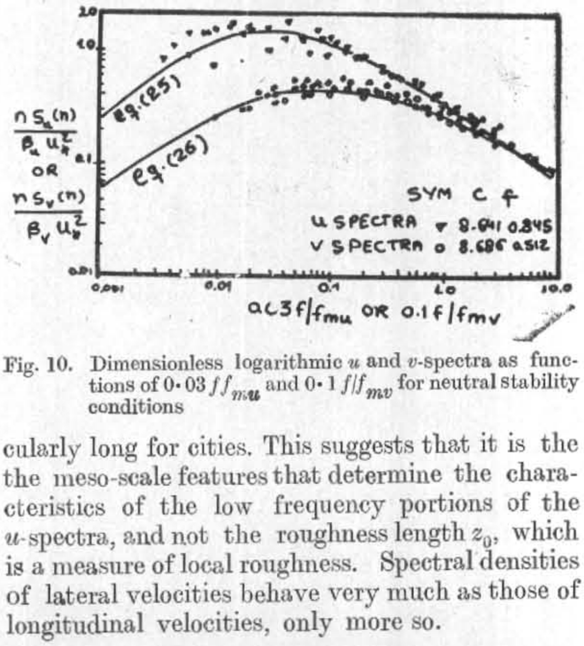

Fig. 10. Dimensionless logarithmic u and v-spectra as functions of $0\cdot03\,f/f_{mu}$ and $0\cdot1\,f/f_{mv}$ for neutral stability conditions

The low frequency portions of u- and v-spectra react to changes in atmospheric stability (Bush *et al.* 1968). For u-spectra energy decreases somewhat as stability increases; for the v-spectra changes are more pronounced. In stable air there is very little energy for frequencies of the order of 1 cycle/min or smaller (Fig. 11 b). Since the energy of the u-components at these wave-lengths is still quite large, 'eddies' in stable or neutral air are elongated along the wind. However, in very stable air, the v-spectra sometimes show gaps between this very low frequency domain and the high frequency mechanical turbulence (Lumley and Panofsky 1964).

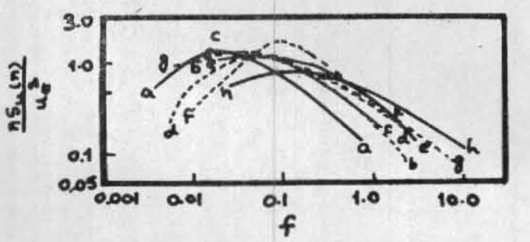

Fig. 11(a). Assorted u-spectra at various locations, (*a*) St. Louis 76m, (*b*) New York 177m, (*c*) Brookhaven 91m, (*d*) South Dartmouth 15 to 46m (neutral and unstable), (*e*) New York city 280 m, (*f*) Montreal 78 m, (*g*) Hanford 386.1m, (*h*) Cape Kennedy 90m and 120 m

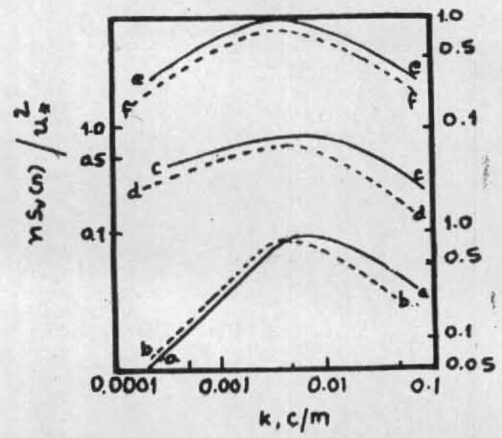

Fig. 11(b). Spectra of lateral velocity at South Dartmouth, Stable : a-46 m, b-91m; Unstable : c-15 and 16 m, d-40 and 46 m; Neutral : e-15 and 16 m, f-40 and 46 m

6. The spectrum of vertical velocity

The spectrum of vertical gustiness has been studied extensively by Panofsky and McCormick (1960). Besides, from recent observations (Pasquil 1971) in the first 100 m above the ground the w-spectrum has been found to have the form shown indicated in Fig. 12. The spectral density is scaled w.r.t. u_*^2 and the characteristic frequency w.r.t. $z/\bar{u}$, as predicted by application of the Monin-Obukhov similarity considerations,

$$nS_w(n)/\sigma^2(w) = G(nz/\bar{u})$$

$$\sigma(w)u_* = \text{Constant} \tag{27}$$

where $G =$ Gust factor

In principle, functions of z/L should be included to allow for the effects of thermal stratification. It appears, however, (*see* Bush and Panofsky 1968) that the simple forms in Eqn. (27) provide an adequate representation not only in neutral conditions but also over a practical range of unstable conditions, with the maximum value of $nS_w(u)/u_*^2$ approximately $0 \cdot 4$ at $nz/\bar{u}$ near $0 \cdot 3$. As regards total energy several independent estimates of $\sigma(w)/u_*$ in neutral and moderately unstable conditions now indicate a value near $1 \cdot 25$.

Panofsky and McCormick have suggested the following empirical formula —

$$\frac{nS_w(n)}{u_*^2} = \frac{6f}{(1+4f)^2} \tag{28}$$

where, f is the ratio of height to wave length. An important distinction between vertical and horizontal gustiness is that the former appears to be strongly dependent on the height; the low frequency part of the z-spectrum as compared to u-spectrum is well defined and reproducible.

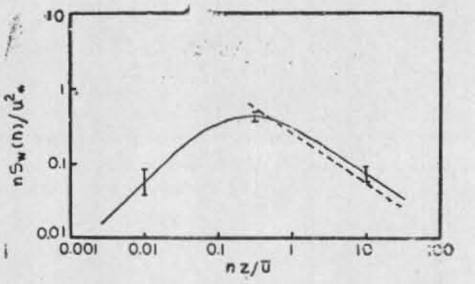

Fig. 12. Micro-meteorological w-spectra in the first 100 m above ground — Eqn. (29)

To sum up, for generalization on the frequency spectrum of the natural wind, the only realistic basis at present appears to be a combination of the similarity ideas with critical empiricism. Unfortunately, while this seems to produce a tolerably satisfactory presentation of the w-spectrum, the case of u- and v-spectrum is still rather confused. The only conclusions that can be drawn for heights upto 100 m are :

(1) The spectral densities on the low frequency side of the peak are especially variable.

(2) The peak of the $nS_u(n)$ spectrum occurs at an equivalent wave-length varying between 300 and 600 m.

(3) On average the spectra on the high-frequency side fits closely to (18),

$$nS_u(n)/u_*^2 = 0 \cdot 26\,(nz/\bar{u})^{-2/3} \tag{29}$$

But individual samples deviate widely from this.

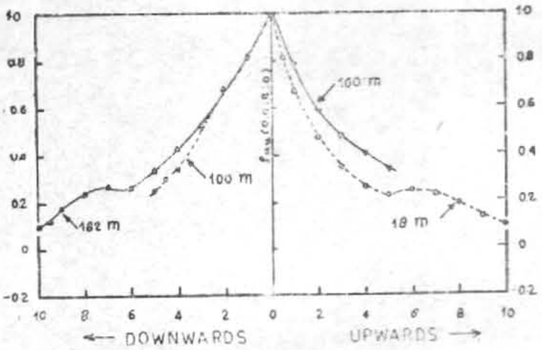

Fig. 13(a). Cross-correlation of along-wind pressure component

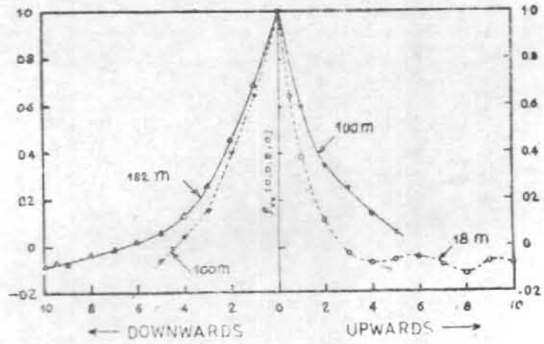

Fig. 13(b). Cross-correlation of cross-wind pressure component

PART III

7. Correlation functions — Space-time structure

Until now, only the simple time average properties of the gust velocity were considered. However, time averages of the turbulent fluctuations of wind speed at one point in space reveal little about the spatial distribution of gusts, which becomes important while considering the wind loading on an extended structure such as a long bridge, tall mast or skyscraper. This can be measured by the cross-correlation coefficient between two velocity measurements separated by a certain distance. The cross-correlation function for zero lag is a measure of how much information is given by a measurement of the gust velocity at one point, about the value of the gust at the same instant of time at some other point. Therefore, if the above function is integrated with respect to the distance between the two points of measurements the result is a length, which represents average extent of the gust size, also referred to as integral length scale of turbulence.

According to Taylor's (1935) hypothesis, space correlations in x-direction with zero time lag are equal to Eulerian time correlations, provided $x = Vt$. Melnichuk (1966) has recently repeated this test of Taylor's hypothesis from an analysis of Doppler radar records of rain at 80 m and showed that the correlation function following the mean motion is not very different from Lagrangian correlation function.

Mathematically, the cross-coveriance function of the gust velocity at the point r and at r' is defined as,

$$C_{ij}(\underline{r}, \underline{r}'; \tau) = \langle v_i(\underline{r}, t) . v_j(\underline{r}, \underline{r}'; t + \tau)\rangle_t \tag{30}$$

and the normalized cross-covariance, also called cross-correlation, as

$$\rho_{ij}(\underline{r}, \underline{r}'; \tau) \; \frac{C_{ij}(\underline{r}, \underline{r}'; \tau)}{\sqrt{C_{ii}(\underline{r}, \underline{r}; o)\, C_{jj}(\underline{r}', \underline{r}'; o)}} \tag{31}$$

where C_{ij} is cross-covariance between ith and jth gust velocity, v_i and v_j are fluctuating velocity in ith and jth directions. ρ_{ij} is cross-correlation function.

Fig. 13 shows the correlation of the longitudinal and the lateral component of the gust velocity as a function of the distance for three different heights (Harris 1968). For the longitudinal component (Fig. 13 a) the general shape of the curves for varying height is the same, although the correlation increases with increasing distance above the ground implying that the length scale (given by the total area under the curve) increases with height. The same holds true for the lateral component (Fig. 13 b) except that the correlation curves for all three levels cross the horizontal axis, and that a considerable region of negative turbulence exists. In this case the corresponding length scales obtained by integration would therefore be the difference between the area under that portion of the curve which lies above the axis, and the area above that portion of the curve that lies below the axis.

Correlation coefficient may also be calculated theoretically. However, one needs to make two simplifying assumptions. The first is the applicability of Taylor's hypothesis, namely that turbulence is convected along by the mean flow velocity, without evolving appreciably in a short distance. The second assumption, which is much more drastic, is that the turbulence is approximately homogeneous isotropic. However, homogeneous isotropic turbulence requires a boundless region and a uniform rate of generation of turbulent energy per unit volume. Clearly, this is not true for a atmospheric turbulence since it arises from the presence of the rough boundary of the earth's surface and is generated at that surface. Nevertheless, it has been found experimentally that at large heights above the earth's surface, the turbulence does tend to become isotropic. Most of the wind loading on a tall structure is determined by the loading on the uppermost third, so for all

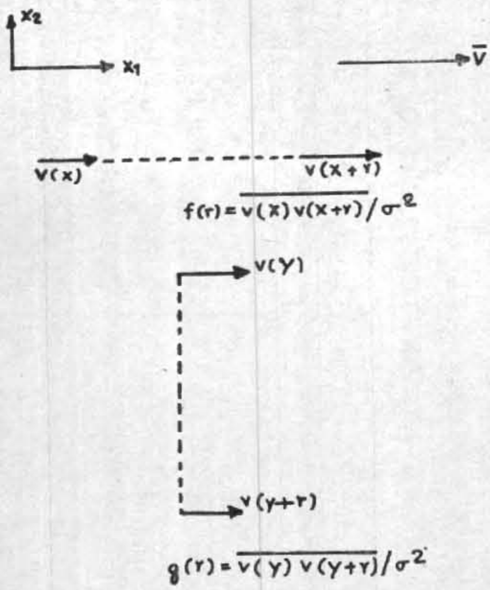

Fig. 14. Illustration of longitudinal and lateral velocity correlations

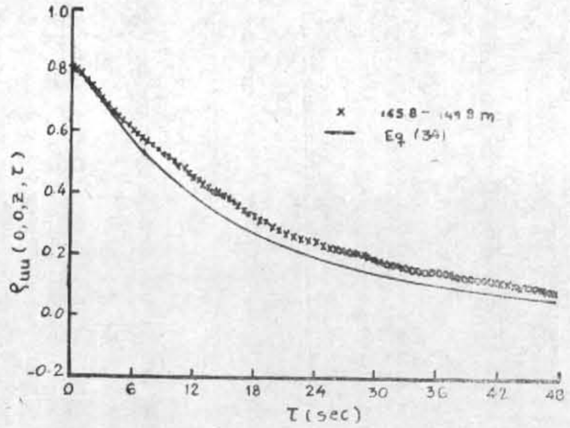

Fig. 15. Cross-correlation between longitudinal components at 165·8 m and at 149·8 m

practical purposes, the assumption of homogeneous isotropic turbulence holds valid. Using Taylor's hypothesis, we may identify the autocorrelation function $\rho(\tau)$ (Eqn. 20) with $f(r)$ (*see* Fig. 14 for definition), as follows,

$$f(r) = \frac{2}{\Gamma(1/3)} \left(\frac{\tilde{r}}{2}\right)^{1/3} k_3 \left(\tilde{r}\right) \tag{32}$$

where $\quad \tau = r/V_z \;\&\; \tilde{r} = \sqrt{2}\,\pi\,\tau\, V_z/V_{10}$

and for homogeneous isotropic turbulence $g(r)$, is related to $f(r)$, by

$$g(r) = f(r) + \tfrac{1}{2}\, r\, \frac{df}{dr} \tag{33}$$

Finally, it follows from spherical symmetry that all the nine auto-and cross-correlations between the various velocity components at two points may be written in terms of $f(r)$ and $g(r)$ according to the relation,

$$\rho_{ij}(r) = \frac{f(r) - g(r)}{r^2}\, s_i\, s_j + g(r)\, \delta_{ij} \tag{34}$$

where δ_{ij} is the Kronecker delta and

$s_i = x_i - x_i'$ and $r^2 = s_i\, s_i$

for $i = j = 1$, we have

$\rho_{ii}(r) = \rho_{ii}(r', r'; \tau)$

The cross-covariance may then be obtained by using the following relationship,

$$C_{ij}(\underline{r}, \underline{r}'; \tau) = \sigma^2(v)\, \rho_{ij}(\underline{r}, \underline{r}'; \tau) \tag{35}$$

Correlation for the longitudinal component of the gust velocity as predicted by Eqn. (34) with the measured values of Harris (1970) for one large height is shown is Fig. 15.

It is obvious that where both the positions considered are at large heights above ground level, the agreement between theory and measured values is good; it became progressively worse nearer to the ground, since nearer to the ground the assumption of homogeneous isotropic turbulence is no longer valid.

Just as the variance could be broken down frequency by frequency into a spectrum, so can the cross-covariance. In the frequency domain the cross-spectrum may be derived by the following relations,

$$S_{ij}(\underline{r}, \underline{r}'; n) = P_{ij}(\underline{r}, \underline{r}'; n) + iQ_{ij}(\underline{r}, \underline{r}'; n) \tag{36}$$

$$P_{ij}(\underline{r}, \underline{r}'; n) = 2 \int_0^\infty [C_{ij}(\underline{r}, \underline{r}'; \tau) + C_{ij}(\underline{r}, \underline{r}'; -\tau)] \cos 2\pi n\tau\, d\tau \tag{37}$$

$$Q_{ij}(\underline{r}, \underline{r}'; n) = 2 \int_0^\infty [C_{ij}(\underline{r}, \underline{r}'; \tau) - C_{ij}(\underline{r}, \underline{r}'; -\tau)] \sin 2\pi n\tau\, d\tau \tag{38}$$

where P_{ij} is the cospectrum (in-phase component) of the cross-spectrum, Q_{ij} is the quadrature spectrum (out-of-phase component) of the cross-spectrum and S_{ij} is the point-spectrum, with

$$S_{ii}(\underline{r}, \underline{r}'; n) = P_{ii}(\underline{r}, \underline{r}'; n) \tag{39}$$

$$Q_{ii}(\underline{r}, \underline{r}'; n) = 0 \tag{40}$$

Since the cross-covariance is not a symmetrical function of τ, the cross-spectrum is a complex quantity. The normalized cross-spectrum obtained by dividing the cross-spectrum by the square root of the product of the appropriate power spectra, may be written as,

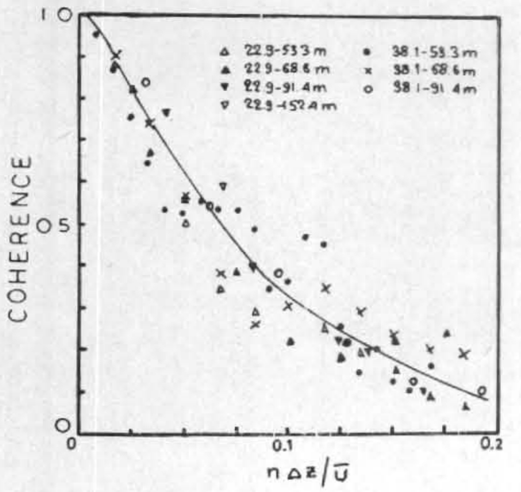

Fig. 16(a). Dependence of coherence on separation between various levels

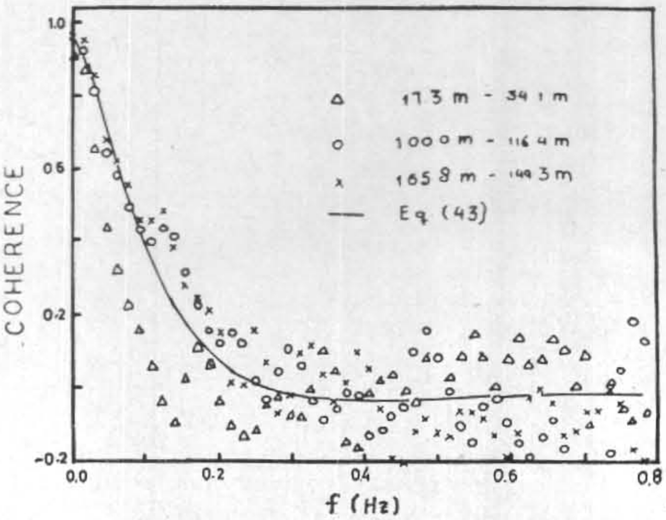

Fig. 16(b). Coherence function for u-component at various levels over Rugby

$$R_{ij}(r, r'; n) = \frac{P_{ij}(r, r'; n) + i\, Q_{ij}(r, r'; n)}{\sqrt{S_{ii}(r, r; n)\, S_{jj}(r', r'; n)}} \qquad (41)$$

The square of absolute value of of the normalized cross-section, *i.e.*, $|R_{ij}(v, r'; n)|^2$ is termed as coherence. The real part of R_{ij} is called the co-coherence and the imaginary part, the quad-coherence.

The existence of the quadrature component can be taken to indicate a preferred orientation of eddies and, therefore, only occurs when there is asmmetry present in the flow. For example there is no significant quadrature component in the cross-wind horizontal cross-spectrum between like components of the velocity; in the vertical direction, however, when there is strong asymmetry, the quad component is non-zero, although not usually as significant as the co-component. For practical purposes it is probably quite adequate to neglect the quad component and take coherence as equal to the square-root of the real part of the normalized cross-spectrum.

Fig. 16(a) shows measurements of coherence taken over terrain of typical roughness for various levels. It is obvious that data for this terrain from different pair of levels fall close to a single curve which approximates to simple exponential form, given by the following relation,

$$\text{Coh}(n) = \exp\left(-C_c n \triangle z / V_{10}\right) \qquad (42)$$

where the value of the coefficient C_c varies from terrain to terrain, *i.e.*, nature of roughness, but *is independent* of the height of measurement.

Coherence may also be calculated theoretically from cross-covariance using the assumption of homogeneous isotropic turbulence. However, in this case the cross-correlations are symmetrical functions of r, so that the normalized cross-spectrum is real, and its square is, therefore, equal to coherence. Under these assumptions, Harris (1970) obtained for the cocoherence the following formula:

$$R\left(s_2, s_3; n\right) = \frac{2}{\Gamma(5/6)}\left\{\left(\frac{\eta}{2}\right)^{5/6} K_{5/6}\left(\eta\right) - \left(\frac{\eta}{2}\right)^{11/6} K_{1/6}\left(\eta\right)\right\} \qquad (43)$$

where $K_{1/6}$ and $K_{5/6}$ are modified Bessel functions of the second kind of order 1/6 and 5/6, and η is given by,

$$\eta = 2\pi\, V_{10} \sqrt{[(s_2^2 + s_3^2)(2 + \tilde{n}^2)]} / \mathbf{L}\, V_z \qquad (44)$$

where $\tilde{n} = n\mathbf{L}/V_{10}$

Fig. 18 (b) shows the measurements of coherence for the longitudinal component as a function of frequency over Rugby for varying height along with the expression (43). The agreement is good at large heights above ground level, but deteriorates for points nearer to the ground. Moreover, it confirms the above observation that coherence is independent of height within the limits of experimental accuracy. For separation in the lateral direction the expression given in Eqn. (42) for coherence is recommended but the value of C_c would be higher in this case. Harris (1970) suggests that expression (43) should be used with $(2+\tilde{n}^2)$ replaced by $(2+4\tilde{n}^2)$ in the definition of η (Eqn. 44).

It was mentioned before that cross-correlation is a numerical measure of the information which is given by a measurement of the gust at one point about the gust at some other point. Physically, gusts are of limited size, and a measurement

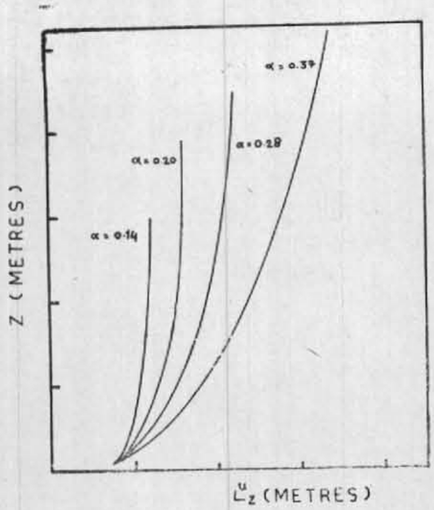

Fig. 17 (b). Length scales of longitudinal components over level terrain of differing roughness

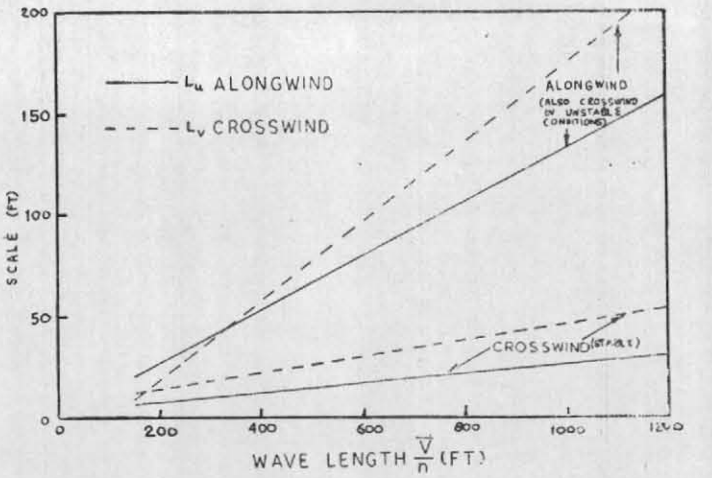

Fig. 17 (b). Along-wind and cross-wind scales of turbulence for the u-and v-components of wind velocity as functions of inverse wave number

of the gust at one point gives only limited information about the value at another point. A measure of the size of the gust, may be obtained by integrating the cross-correlation for zero lag; this is also referred to as the integral length scale of turbulence.

Mathematically it may be defined as,

$$L^i_{xi} = \int_0^{\infty} \rho_{ii}(x_i, x_i; o)\, dr \tag{45}$$

where the superscript i refers to the component of gust velocity being measured and x_i denotes the axis of separation of the two points of measurements. Thus three length scales can be defined for each gust component with respect to the three directions in space. Thus for the longitudinal component, using the definition of $f(r)$ and $g(r)$ (Fig. 14) the three length scales are given by,

$$L^u_x = \int_0^{\infty} f(r)\ dr \tag{46}$$

$$L^u_y = L^u_z = \int_0^{\infty} g(r) dr = \tfrac{1}{2}\ L^u_x \tag{47}$$

Similarly, we can define length scales for the other two components of the gust velocity using Taylor's hypothesis. These length scales can be related to the time scale of the standard gust-spectrum by,

$$L^u_z = V_z\ T = 0.084\ \mathbf{L}\, V_z/V_{10}$$

$$= 151(z/10)^a \tag{48}$$

$$L^v_z = L^w_z = \tfrac{1}{2} L^u_z = 75.5\ (z/10)^a \tag{49}$$

TABLE 1

Variation of length scales with height at Rugby

Height (m)	L_w+ (m)	L_w^- (m)	$\frac{1}{2}L_u$ (m)
18	57	9*	84
100	68	50	113
182	74*	71	126

These equations imply that the length scales are related to the height above the ground and the roughness of the terrain and that the length scales increase with height at the same rate as the mean wind speed. Panofsky and Singer (1965) have suggested that the vertical integral scales are proportional to $z^{2/3}$. Fig. 17(a) shows the change of scale length with height for different terrains [the values of α used are those suggested in Table 2 (Pt. I)].

Measurements of L^u_z at Rugby have confirmed the values given for an open country site. It should be noted that L^v_z and L^w_z will only be equal to $\frac{1}{2}L^u_z$ for homogeneous isotropic turbulence. Nearer to the ground $L^u_z\ /\ L^v_z$ will be higher. The available data indicate that instable and neutral conditions the cross-wind integral scale of the u-component L^u_y is less than the alongwind integral scale L^u_x by a factor of six (Panofsky 1962). In the case of L^u_z the asymmetry in the flow created by the presence of the earth's surface gives rise to two values of L^u_z at each height, depending upon whether the integration of the cross-correlation is carried out with respect to vertical separation upwards L^u_{z+} or downwards L^u_{z-}. Based on the correlation measurements given in Fig. 13, the appropriate values of the corresponding length scales are shown in Table 1. The values marked '*' are estimated because of lack of experimental data.

Fig. 17(b) shows Cramer's (1959) measurements of the along-wind and cross-wind scales of the u-and v-components of the gust vector. These suggest that the along-wind scales of both the along-wind and cross-wind velocity components (L_x^u and L_x^v) are roughly 1/6 of the wave-length in both stable and unstable atmospheric conditions. In unstable conditions the transverse scales of the same two velocity components are again roughly the same but slightly smaller being 1/10 of the wave-length. In stable conditions the cross-wind peaks are very much less than the along-wind being roughly 1/40 and 1/25 of the wave-length for the along-wind and cross-wind components respectively.

The indication this gives is that in unstable conditions the along-wind and cross-wind scales are about equal (and equal to 1/6-1/8 of the wave-length), and in stable conditions the eddies are very much elongated in the direction of the wind and the cross-wind scales are of the order of 1/3-1/5 of the along-wind scale which is itself equal to roughly 1/8 of the wave-length. Majority of evidence suggests that the elongated eddy model is more representative.

Furthermore, because of wind shear, its major axis is not aligned with the mean flow direction, but points upwards forming an angle with the horizontal. In other words, a gust is experienced at the top of a high tower before its base. It is obvious from Fig. 18 that shear slopes defined by $\triangle x/\triangle z$ are always larger for the lateral component v than for longitudinal component u. Generally the slopes vary between 0·5 and 1 for the u-components and between 1 and 3 for the v-components. They show a tendency to decrease with height. This is also confirmed by the results of Grant (1958) who also found that the longitudinal scale was 7 to 8 times larger than the lateral. It may be concluded that in stable and neutral conditions L_x^u is greater than L_y^u by a factor of 7, and in convective (light wind, unstable) conditions the difference is slight and probably negligible as a rough approximation.

For the practical application of these concepts, one must consider that this generalization only applies above regularly rough surface, which means above the roofs of the buildings in an urban area. Below this level, the flow will be a composite of wakes, deflections, and channelling, local effects produced by the buildings and

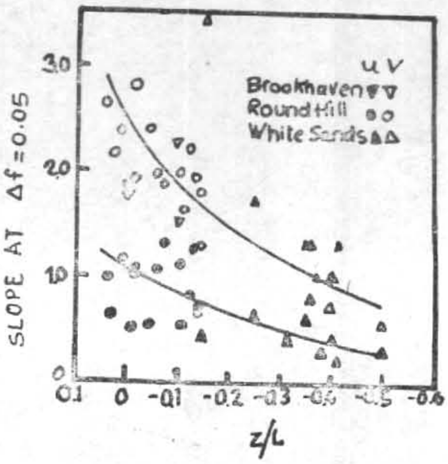

Fig. 18. Slope of eddies for the u-and v-components of the wind as function of of z/L

their relative position, a situation precluding any possible form of generalization.

8. Gust Factors

Wind speeds used in current design specifications are based on mean wind speed observations multiplied by a constant gust factor to allow for the fluctuations in the wind speed. However, this procedure neglects both the dynamic properties and the size of the structures. Moreover, assuming a constant gust factor is equivalent to assuming that the intensity of turbulence is identical for all sites. The results given above show that this is obviously incorrect. Further, the maximum wind speed also varies with the time over which it is averaged. Thus, the gust factor should also be related to the time with the shorter time gusts being more important for certain loading, as for example in claddings, etc, than the longer time gusts.

The gust factor G is defined as,

$$G = u/\bar{u} \tag{50}$$

where u is the peak wind speed within a data record of length t in time and ū is the mean wind speed associated with the record. If σ denotes the variance of the fluctutations of velocity about he mean, then $u+3\sigma$ is an estimate of the peak wind speed; thus we may write,

$$G = 1 + 3\,\sigma/\bar{u} \tag{51}$$

where σ is related to the friction velocity u_*, through

$$\sigma = A(R_i, t)\; u_* \tag{52}$$

where σ is a function of the Richardson number R_i and the averaging time t.

It was shown before that the natural boundary layer profile may be represented by a power law for simplicity as opposed to a logarithmic

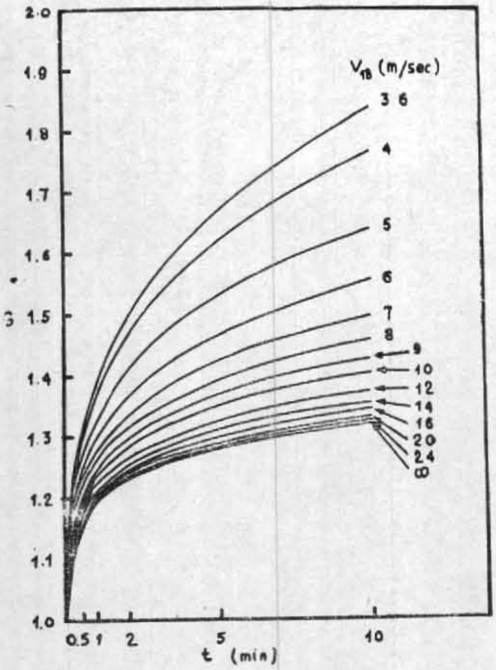

Fig. 19 (a). The gust factor at the 18m level as a function of the averaging time for various peak wind speeds

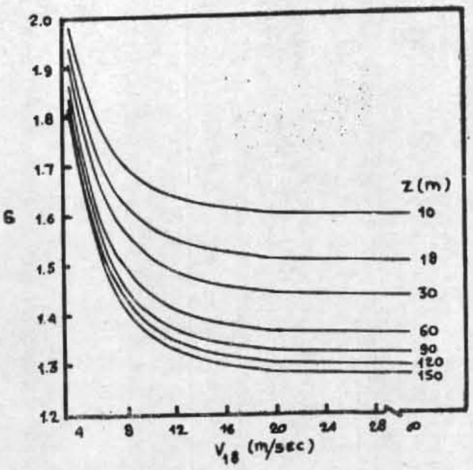

Fig. 19 (b). The gust factor as a function of the peak wind speed at the 18m level for various heights, associated with a 10-minute grand average

law. However, in the surface layer (the first 30 metres of the boundary layer) the wind profile is best given by,

$$\bar{u} = \frac{u_*}{k} \ln \left[\frac{z}{z_0} - \Psi (R_i) \right] \tag{53}$$

where $k=0\cdot4$, z_0 is the surface roughness length and $\Psi\ (R_i)$ is a universal function of R_i. For neutral condition $R_i=0$ and hence Ψ vanishes. Combining the above equations, we get,

$$G = 1 + \frac{3kA\ (Ri, t)}{\ln z/z_0 - \Psi\ (Ri)} \tag{54}$$

In neutral atmosphere we have,

$$G = 1 + \frac{3kA\ (t)}{\ln z/z_0} \tag{55}$$

As the averaging time decreases, the variation will decrease so that A is a decreasing function of the averaging time and thus G is an increasing function of the averaging time. Furthermore, it is obvious from Eqn. (54) that the gust factor decreases as the height increases. As the air becomes more stable, R_i decreases and hence the gust factor increases.

Fichtl *et al.* (1970) developed a gust factor model for the Kennedy Space Centre with 181 hours of turbulence data encompassing a broad range of wind conditions. Fig. 19 (a) shows the dependence of the 18-metre level gust factor on the averaring time and the peak wind speed and Fig. 19 (b) shows the dependence of the 10-minute gust factor on the peak wind speed and height. Here the peak wind speed at the 18-metre level plays the role of a stability parameter. Within the range of variation of the data, the 1-hour gust factor and the 10-minute gust factor are approximately equal, confirming the earlier observation that the spectrum of the horizontal wind speed near the ground is characterized by a broad energy gap centred at a frequency approximately equal to 1 cycle/hour.

It is noted from above that the gust factor varies with the averaging time period, the site conditions and with height above ground level. Another way to represent the collective effects of these various parameters is to express the gust factor in terms of the turbulence intensity $\sigma/\bar{u}$.

Mackey (1970) obtained the following expression for the gust factor $[\bar{G}(t/T)]$ in terms of turbulence intensity.

$$G\ (t/T) = 1.06226\ (\sigma/\bar{u})^{1\cdot2716} \log\ (t/T) \tag{56}$$

Using the above equations and adopting the values of $0\cdot26$, $0\cdot16$ and $0\cdot08$ for the turbulence intensity in urban areas, open country and open sea-front areas respectively, Table 2 shows the computed gust factors for various averaging periods. It should be noted that Eqn. (56) applies

TABLE 2

Theoretical gust factors for various averaging periods

$G\ (t/T)$ $T=3600$ sec	Gust period t (sec)								
	3600	600	300	60	30	10	5	3	1
Urban area $\sigma/V=0 \cdot 26$	1·00	1·202	1·279	1·461	1·538	1·662	1·738	1·797	1·922
Open country $\sigma/V=0 \cdot 16$	1·00	1·108	1·150	1·248	1·290	1·356	1·398	1·430	1·496
Open sea $\sigma/V=0 \cdot 08$	1·00	1·047	1·062	1·102	1·120	1·147	1·164	1·177	1·205

to wind velocities determined at a single point in space.

For the design of most engineering structures which are sensitive to wind, determination of the gust factor at a single point in space is insufficient. For tall slender towers and point-block, high-rise buildings, for example, a knowledge of variation of gust factor with height is vital to economic design, whereas for long span bridges, slab-type buildings and overhead conductors variation of gust factor in a horizontal plane may be the dominant consideration. Estimates of the variation of gust factor with height can be obtained but the knowledge of the variation of the gust factor in a horizontal plane is practically non-existence.

9. Conclusions

From the above the following conclusions may be drawn :

The entire wind spectrum may be divided into three regions : the macro-meteorological region, the meso-meteorological region and the micro-meteorological region (the region of greatest importance to us).

The r.m.s. gust speed decreases very slowly with height in the lower part of the natural boundary layer.

At high mean wind speeds the spectral peak appears to exists at wave numbers between $0 \cdot 001$ and $0 \cdot 002$ cycles m^{-1} and the peak wave length appears to be independent of the type of the surface. In the high frequency range, quite close to the ground, observations indicate greater energy in the longitudinal component than in the vertical components of fluctuations.

u- and v-spectra show a greater dependence on the type of terrain suggesting that meso-scale features are of importance for the low frequency portion. The low frequency portion of u- and v-spectra react to changes in atmospheric stability with the v-spectrum being more sensitive to atmospheric stability. The w-spectrum follows the similarity theory the most out of the three components and shows a marked dependence on height.

Based on measurements of cross-correlation and other results, tentative conclusions are derived about length scales. It is suggested that the length scales are related to the height above the ground and the roughness of the terrain and that the length scales increase with height at the same rate as the mean wind speed.

The gust factor varies with the averaging time period, the site conditions and with height above the ground. The gust factor decreases with increasing height and increases with increasing surface roughness and atmospheric stability.

Nomenclature

$C(t)$ Auto-covariance

G_{ij} Cross-covariance between i th and j th gust velocity

c_p Specific heat of air at constant pressure

C_u, C_v Empirically determined parameters occurring in formulae of power spectra

f Non dimensional frequency $(=nz/\bar{u})$

$f(r)$ Basic correlation function

f_{mu}, f_{mv} Value of f associated with peaks of logarithmic u- and v-spectrum

g Acceleration due to gravity, or a subscript denoting geostrophic value

$g(r)$ Basic correlation function

$G, G(t/T)$ Gust factor

H Vertical turbulent heat flux, positive upward

k Von Karman constant

K Surface drag coefficient

L Monin-Obukhov length

L Integral length scale

L^i_{xi} Length scale of the i gust component in x_i-direction

m metre

n Frequency in cycles per second

P_{ij} Real part of cross-spectrum

Q_{ij} Imaginary part of cross-spectrum

r_u, r_v Empirically determined parameters occurring in formulae of power spectra

R_i Richardson number

R_{ij} Coherence

$S(n)$ Spectral density at frequency n

$S_u(n)$ $S_v(n)$, $S_w(n)$ Power spectra of the u-, v- and w-components

S_{ij} Cross-spectrum

T Absolute temperature, total time during which signal value is averaged

u Peak wind speed in x-direction

u_* Friction velocity $[=\sqrt{(\tau_o/\rho)}]$

u', v', w' Fluctuating wind speed in x, y, z directions

$\bar{u}, \bar{v}, \bar{w}$ Mean wind speed in the along-wind, across-wind and the vertical directions respectively

$\underline{v}$ Total fluctuating velocity

v_i Fluctuating velocity in the ith direction

V_z Mean wind speed at height z

V_{10} Mean wind speed at height of 10 metres.

x $n\mathsf{L}/V_{10}$

z Distance in the vertical direction

z_0 Surface roughness length

mph Miles per hour

r.m.s. Root-mean-square

w.r.t. With respect to

α Power law exponent

β_u Vertical collapsing factor for power spectra for u-component

β_v Vertical collapsing factor for power spectra for v-component

ϵ Rate of dissipation of turbulent kinetic energy per unit mass

φ_m Monin-Obukhov stability function for momentum

$\sigma(u)$, $\sigma(v)$, $\sigma(w)$ Variance of u, v and w components of fluctuating velocity

$\sigma(\underline{v})$ Variance of total fluctuating velocity

τ Horizontal shearing stress, time lag

ρ Air density

ρ_{ij} Cross-correlation function

$\rho(\tau)$ Auto-correlation coefficient

Ψ Logarithmic wind profile stability defect.

REFERENCES

Berman, S. 1965 'Estimating the longitudinal wind spectrum near the ground', *Quart., J.R. Met. Soc.*, **91**, pp. 301-317.

Bush, N. E., Frizzola, J. A. and Singer, I. A. 1968 'The micrometeorology of the turbulent flow field in the atmospheric surface boundary layer', Act a Poly, Scand. Phy. including Nucleonics Ser., Ph. No. 59.

Bush, N. E. and Panofsky, H. A. 1968 *Quart. J. R. Met. Soc.*, **94**, pp. 132-148.

Cramer, H. E. 1959 'Measurements of turbulence structure near the ground within the frequency range from 0·5 to 0·01 cycles /sec', *Adv nces in Geophysics*, Academic Press, New York.

Davenport, A. G. 1961 *Quart. J. R. Met. Soc.*, **87**, pp. 194-211.

1962 'Buffetting of a suspension bridge by storm winds', J. Str. Dvn., *Proc. ASCE*, 88, pp. 233-267.

REFERENCES (contd)

Deland, R. J. and Panofsky, H. A.	1957	'Structure of turbulence at O'Neil, Nebraska and its relation to the structure at Brookhaven', The Penn. State Univ. Sci. Rep. No. 2.
Fichtl, G. H. and McVehil, G. E.	1969	'Longitudinal and lateral spectra of turbulence in the atmospheric boundary layer', Agard CP No. 48.
Fichtl, G. H., Kaufman, J. W. and Vaughan, W. W.	1970	Building Science Series 30, pp. 27-41.
Grant, H. L.	1958	*J. Fluid, Mech.*, **4**, pp. 149-170.
Harris, R. I.	1968	'Measurements of wind structure at heights upto 598 ft above ground level', Symp. on wind effects on buildings and structures, Loughborough.
	1970	'The nature of the wind', A CIRIA Seminar on 'The modern design of wind sensitive structures', London.
Lumley, J. L. and Panofsky, H. A.	1964	*The structure of atmospheric turbulence*, John Wiley and Sons, New York.
Mackey, S.	1970	*Ind. Aerodynamics Abstracts*, **1**, pp. 1-16.
Melnichuk. Y. V.	1966	*Izv. Atmos. & Ocean. Phy.* **2**, pp. 695-704.
Monin, A. S.	1959	*J. geophys. Res.*, **64**, pp. 2196-2197.
Panofsky, H. A.	1962	*Quart. J.R. Met. Soc.*, **88**, pp. 57-69.
	1969	'The structure of atmospheric shear flows', Agard CP No. 48.
Panofsky, H. A. and McCormick, R. A.	1960	*Quart. J.R. Met. Soc.*, **86**, pp. 495-503.
Panofsky, H. A. and Singer, I. A.	1965	*Ibid.*, **91**, pp. 339-344.
Pasquill, F.	1971	*Phill. Trans. Roy. Soc. London*, **A269**, pp. 439-456.
Prasad, B. and Panofsky, H. A.	1967	'Properties of variance of the meteorological variables at Round Hill', Report No. ECOM-0035-F, Penn. State Univ.
Taylor, G. I.	1935	*Proc. Roy. Soc. Lond.*, **151A**, pp. 421-476.
Van der Hooven, I.	1957	*J. Met.*, **14**, pp. 160-167.
Columbia Univ. Press.	1949	*Tables of Bessel function of fractional order*, **11**.